ROYAL SOCIETY OF CHEMISTRY

EDGE ARTICLE

Check for updates

All publication charges for this article have been paid for by the Royal Society of Chemistry

Cyclopropylmethyl *S*-adenosyl-ʟ-methionine: an enzymatic cyclopropylmethyl donor

Huimin Zhao,[a] Nanhai Yu,[a] Sican Wang[a] and Min Dong [ID] *[abc]

The cyclopropylmethyl group has been valued in medicinal chemistry for its stereoelectronic properties in optimizing drug stability and target affinity. Selectively introducing a cyclopropylmethyl group is a challenge in organic synthesis. Here, we developed an enzymatic approach using a cyclopropylmethyl-*S*-adenosylmethionine analogue (CPM-SAM) and methyltransferases. CPM-SAM was prepared using an engineered *Acl*HMT from iodomethyl-cyclopropane and *S*-adenosylhomocysteine. Enzyme cascades with engineered *N*-, *S*-, *C*-, and *O*-methyltransferases selectively cyclopropylmethylate diverse substrates under mild conditions. This strategy demonstrates the potential of SAM analogues and engineered methyltransferases in the late-stage incorporation of cyclopropylmethyl groups into bioactive molecules.

Introduction

The cyclopropylmethyl (CPM) group has emerged as a pivotal functional group in medicinal chemistry, leveraging its unique structural features to increase drug specificity,[1] refine target-binding patterns,[2] and optimize hydrophobicity profiles.[3] The characteristic high angle strain of cyclopropane confers metabolic advantages by reducing accessibility to enzymatic attack, thereby decreasing hepatic clearance rates and prolonging plasma half-life through improved metabolic stability.[4] Currently approved drugs containing the cyclopropylmethyl group (Fig. 1) show broad therapeutic applications. Key examples include nalmefene[5] (an opioid antagonist for addiction) and roflumilast[6] (a phosphodiesterase 4 inhibitor). Furthermore, multiple investigational candidates are in preclinical development, exemplified by the GlyT1-selective inhibitor DCCCyB,[7] alongside clinical-stage agents such as pomotrelvir, a SARS-CoV-2 main protease (Mpro) inhibitor undergoing evaluation for COVID-19 treatment.[8]

However, the synthetic challenges associated with selective CPM incorporation remain significant. *In situ* cyclopropanation needs harsh conditions (strong Lewis acids, high heat, or metal catalysts), risking ring-opening, side reactions and environmental impact.[9,10] Therefore, developing green, efficient enzymatic strategies for the selective incorporation of pre-formed cyclopropane groups (*e.g.*, CPM) bypasses C–C bond inertness[11] and circumvents direct cyclization challenges. This approach would advance the preparation of cyclopropane-based pharmaceuticals for next-generation therapeutics with optimized pharmacokinetics and enhanced target engagement.

S-Adenosyl-ʟ-methionine (SAM or AdoMet), a ubiquitous cofactor in living organisms, serves as the primary methyl donor for methyltransferases to methylate diverse biomolecules, including DNA, RNA, proteins, and small-molecule metabolites. This biochemical process underlies a variety of basic biological functions.[12] The versatility of SAM-dependent methyltransferases (MTs) has driven extensive exploration of synthetic SAM analogs with modified methyl substituents.[13–15] Recently, this repertoire was further expanded to enzymatic transfer of fluoroalkyl groups, such as fluoromethyl,[16–20] fluoroethyl,[21] and other fluoro-containing functional groups[22] that are important in medical chemistry and agrochemistry. Given the
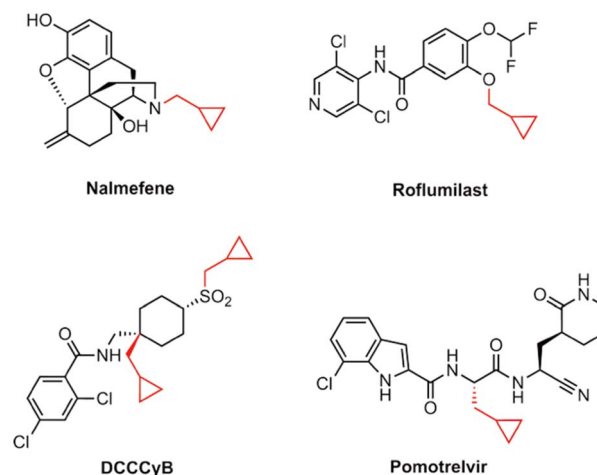
[a]State Key Laboratory of Synthetic Biology, Frontiers Science Center for Synthetic Biology, School of Chemical Engineering and Technology, Tianjin University, Tianjin 300072, China. E-mail: mindong@tju.edu.cn

[b]School of Synthetic Biology and Biomanufacturing, Tianjin University, Tianjin 300072, China

[c]Haihe Laboratory of Sustainable Chemical Transformations, Tianjin 300192, China

Fig. 1 Drugs containing cyclopropylmethyl groups.

pharmacological significance of cyclopropylmethyl groups in drug design, we propose the development of cyclopropylmethyl-SAM (CPM-SAM) as a novel cyclopropylmethyl donor for enzymatic cyclopropylmethylation. On the basis of our work with a fluoroethyl transfer reaction, in which several methyltransferases cannot tolerate the size of the fluoroethyl group and need protein engineering, the use of the bulkier cyclopropylmethyl would be a challenge for both SAM analogue synthesis and methyltransferases.
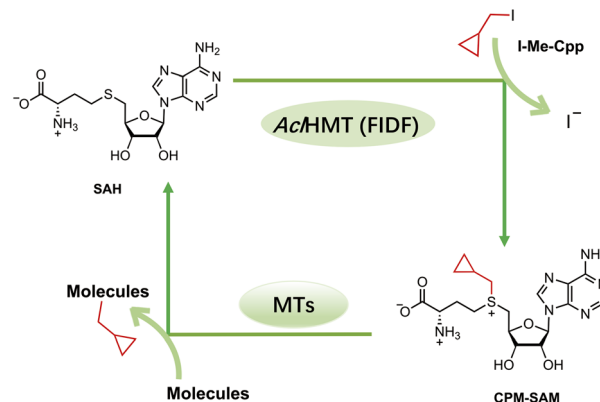
Results and discussion

Synthesis of CPM-SAM

Halide methyltransferases (HMTs) have been used for SAM analogue preparation.[23] We heterologously expressed three phylogenetically distinct HMTs, *vpa*HMT, *uma*HMT, and *Acl*HMT, to evaluate their capacity for CPM-SAM synthesis from *S*-adenosyl-L-homocysteine (SAH) and iodomethyl-cyclopropane (I-Me-Cpp, Scheme 1). HPLC and LC-MS analyses detected trace amounts of CPM-methylthioadenosine (CPM-MTA, a degradation product of CPM-SAM, Fig. S2 and S3) in reactions containing *vpa*HMT or *uma*HMT. Notably, both CPM-MTA and CPM-SAM were detected in the *Acl*HMT-catalyzed reaction (Fig. S2). These findings demonstrate that *Acl*HMT exhibits slightly better tolerance toward iodomethylcyclopropane (I-Me-Cpp) moieties, albeit with compromised catalytic efficiency. A systematic enzyme engineering study on *Acl*HMT by Hammer et al.[24] developed an *Acl*HMT mutant (V11F/L30I/L39D/W41F), demonstrating high activity toward I-Me-Cpp in SAM analogue synthesis. Therefore, we utilized *Acl*HMT (V11F/L30I/L39D/W41F), denoted as *Acl*HMT (FIDF), to synthesize CPM-SAM (Fig. S2). CPM-SAM was successfully prepared with 61.5% yield, significantly higher than that of the chemical method (17.32% yield, see the SI). CPM-SAM was fully characterized by high-resolution mass spectrometry (HRMS), ^{1}H and ^{13}C NMR. Additionally, owing to its tendency to decompose into the MTA analogue, we evaluated the stability of CPM-SAM in buffers at pH 1.0 and 7.0, revealing degradation rates of 2.1% and 16.2% to CPM-MTA, respectively, after 24 hours at 30 °C (Fig. S3).

*Acl*HMT (FIDF)–methyltransferase cascade catalyzed cyclopropylmethylation

After successfully obtaining CPM-SAM, we aimed to investigate whether CPM-SAM can be recognized by SAM-dependent MTs to cyclopropylmethylate diverse compounds. Enzymatic cascade reactions of HMTs and MTs, developed by Seebeck[16] and later effectively used in fluoroalkylation,[18,21] were used for CPM-SAM-mediated cyclopropylmethylation (Scheme 2). Nicotinamide *N*-

Scheme 2 Enzyme cascade of *Acl*HMT (FIDF) and methyltransferase for cyclopropylmethyl transfer reactions.

methyltransferase (NNMT) is a key enzyme in nicotinamide (NCA, **1**) metabolism and xenobiotic detoxification. Its metabolite, 1-methylnicotinamide, protects against lipotoxicity-induced renal tubular injury.[25] Only trace amounts of cyclopropylmethylated NCA (**2**, 3.1% yield) were detected in the *Acl*HMT (FIDF)–NNMT cascade reaction (Fig. 2 and S6A). The low activity may stem from steric constraints of the large cyclopropylmethyl group of CPM-SAM, which requires an expanded active pocket. By analyzing the crystal structure of NNMT with SAH bound (PDB: 2IIP), we identified two residues near the sulfur atom of SAH that likely influence substrate binding: Y11 and Y204 (Fig. S5A). Subsequent docking analysis
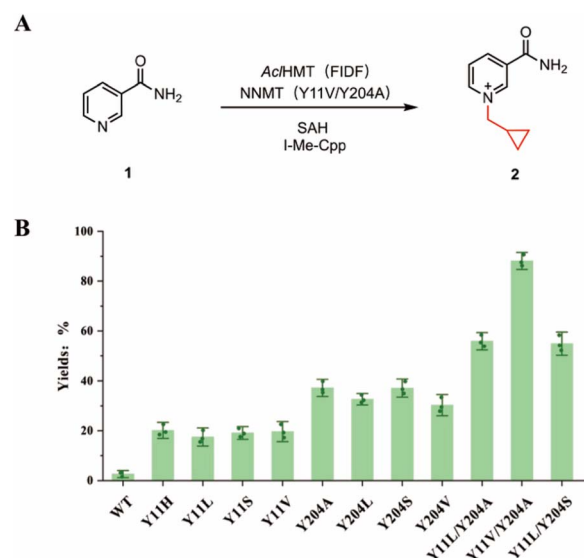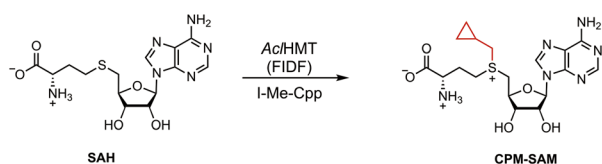
Fig. 2 (A) Cyclopropylmethylation activity of the *Acl*HMT (FIDF)–NNMT (Y11V/Y204A) cascade reactions. The *Acl*HMT (FIDF)–NNMT (Y11V/Y204A) assay contained 80 μM SAH, 3 mM I-Me-Cpp, 1 mM NCA (**1**), 40 μM *Acl*HMT (FIDF) and 80 μM NNMT (Y11V/Y204A) in 200 mM sodium phosphate (pH 7.0), and the solution was incubated at 30 °C for 24 h. (B) Activity summary of *Acl*HMT (FIDF)–NNMT cascade reactions with NNMT mutants. The data plotted are the means of three independent measurements with standard deviation.
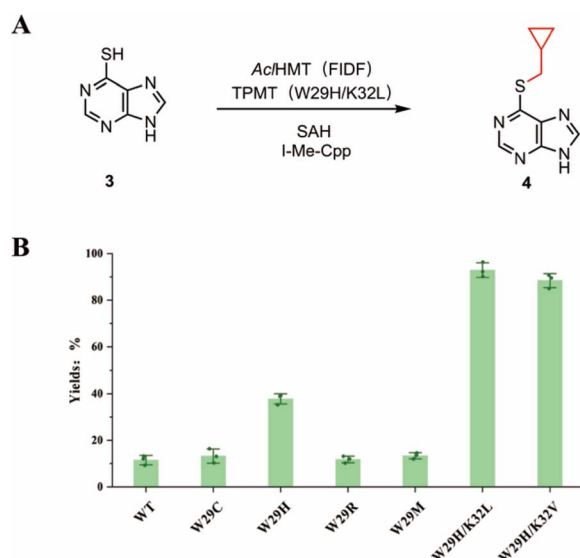
Scheme 1 Synthesis of CPM–SAM.

of CPM-SAM with NNMT revealed residue Y204 positioned 1.1 Å from the cyclopropylmethyl group and residue Y204 2.6 Å from the purine ring of CPM-SAM (Fig. S6B and C). We then generated Y11A/H/L/S/V and Y204A/H/L/S/V single mutants and assessed their catalytic activity. The Y204A mutant exhibited the highest activity. We then constructed several double mutants and Y11V/Y204A achieved a reaction yield of 89.52%, which is 29-fold higher than that of the wild-type and also much higher than that of the chemical method of 65.2% yield (Fig. 2 and page S6). Molecular docking of CPM-SAM with NNMT (Y11V/Y204A) confirmed the improved accommodation of the cyclopropylmethyl group within the active site (Fig. S5D). Time-dependent experiments were conducted to evaluate both direct catalysis by NNMT (Y11V/Y204A) on CPM-SAM and cascade catalysis involving AclHMT (FIDF)–NNMT (Y11V/Y204A). Compared with direct catalysis, the cascade system demonstrated a slightly superior product yield, which was likely attributed to the inherent instability of CPM-SAM (Fig. S6C). Kinetic analysis revealed that the NNMT (Y11V/Y204A) mutant exhibits comparable K_M values for SAM and CPM-SAM, while its k_{cat} value decreased by a factor of 35 with CPM-SAM (Table S3).
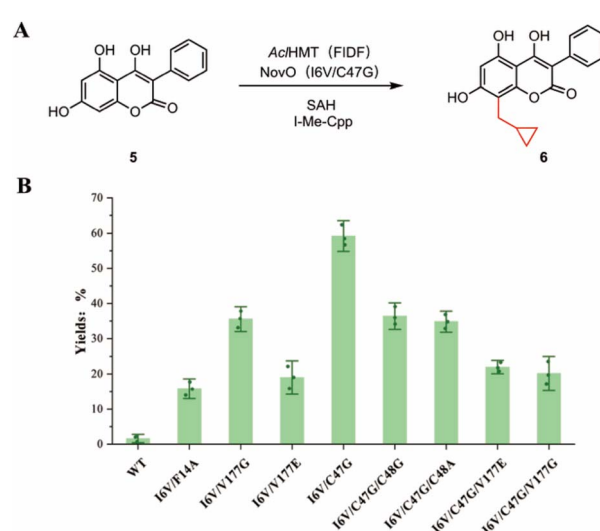
We further explored the catalytic activity of S-methyltransferase toward CPM-SAM. Thiopurine S-methyltransferase (TPMT) catalyzes the S-methylation of thiopurines and thiopyrimidines. This is a key metabolic pathway for thiopurine drugs like 6-mercaptopurine (6-MP), 6-thioguanine (6-TG), and azathioprine, which are currently used for the treatment of childhood acute lymphoblastic leukemia, autoimmune diseases, inflammatory bowel disease, and transplant rejection.[26] We evaluated the activity of the AclHMT (FIDF)–TPMT

cascade system for the cyclopropylmethylation of 6-mercaptopurine (6-MP, 3, Fig. 3 and S8), achieving a 12.07% yield of the cyclopropylmethylated product (4, Fig. 3B). To increase the catalytic efficiency, structural analysis of TPMT with SAH bound (PDB: 2BZG) revealed that residue W29 might have steric space with the cyclopropylmethyl group (Fig. S7B). Saturation mutagenesis of W29 identified the W29H variant that significantly improved catalytic activity (yield 38.9%, Fig. 3B). Given that AclHMT belongs to the TPMT family, we extended our successful engineering strategy of AclHMT to TPMT. Sequence alignment identified three equivalent positions: W29/K32/F40 in TPMT corresponding to W27/L30/W41 in AclHMT (Fig. S7A). Double mutants through the combinatorial pairing of W29H with K32 and F40 were prepared. Notably, the TPMT (W29H/K32L) variant demonstrated significantly enhanced performance with a yield of 92.3% (7.6-fold higher than that of the wild-type enzyme, Fig. 3B). This enhancement likely stems from the W29H mutation accommodating CPM-SAM through optimized spatial arrangement, while maintaining the capacity to form an aromatic lid at the binding site.[27]

Following successful CPM-SAM-mediated cyclopropylmethylation on small molecules, we extended this method to achieve late-stage selective modification of complex pharmaceuticals and natural products. Coumarins are natural products produced in plants and some microbes. Coumarins and their derivatives are widely used in pharmaceuticals with anti-inflammatory, anti-ulcer, antitumor, antimicrobial, and anticoagulant activities.[28,29] NovO catalyzes the regioselective C8-methylation of coumarin.[30] Using 4,5,7-trihydroxycoumarin (5) as the substrate, we evaluated the cyclopropylmethylation

Fig. 3 (A) The AclHMT (FIDF)–TPMT (W29H/K32L) assay contained 80 μM SAH, 3 mM I-Me-Cpp, 4 mM TCEP, 1 mM 6-mercaptopurine (3), 40 μM AclHMT (FIDF) and 80 μM TPMT (W29H/K32L) in 200 mM potassium phosphate buffer (pH 8.0), and the solution was incubated at 30 °C for 24 h. (B) Activity summary of AclHMT (FIDF)–TPMT cascade reactions with TPMT mutants. The data plotted are the means of three independent measurements with standard deviation.

Fig. 4 (A) Cyclopropylmethylation activity of the AclHMT (FIDF)–NovO (I6V/C47G) cascade reactions. The cascade reaction mixture contained 80 μM SAH, 3 mM I-Me-Cpp, 1 mM substrate (5), 40 μM AclHMT (FIDF) and 80 μM NovO (I6V/C47G) in 200 mM sodium phosphate (pH 7.0), and the mixture was incubated at 30 °C for 24 h. (B) Activity summary of AclHMT (FIDF)–NovO cascade reactions with NovO mutants. The data plotted are the means of three independent measurements with standard deviation.

activity of the *Acl*HMT (FIDF)–NovO enzyme cascade (Fig. 4 and S10). As anticipated, NovO (WT) exhibited poor tolerance toward CPM-SAM, with only trace amounts of cyclopropylmethylated products detected (**6**, yield 2%, Fig. 4B). Structural analysis of NovO (SAH-bound, PDB: 5MGZ) revealed that residues I6 and F14, located 3.9 Å and 5.1 Å from the sulfur atom respectively (Fig. S9A), might create steric hindrance for CPM-SAM binding. Molecular docking of CPM-SAM into NovO further demonstrated spatial overlap between the cyclopropylmethyl group and substrate 5 (Fig. S9B). FuncLib[31] analysis of the residues within a 4 Å radius of CPM-SAM in the CPM-SAM–NovO docking complex suggested the mutation of C47 (3.3 Å from the purine ring) to glycine and C48 to alanine or glycine, along with the distal residue V177 to glutamic acid or glycine. Subsequent docking simulations of the CPM-SAM–NovO (I6V/C47G) variant demonstrated resolved substrate overlap, with CPM-SAM reoriented properly. The C47G mutation facilitated optimal bending of CPM-SAM to approach the C8 position of the substrate (Fig. S9C and D). We subsequently generated single and combinatorial mutants at these five sites. Activity assays revealed that NovO (I6V/C47G) was the most efficient variant, achieving a 58.48% yield with a 28-fold increase over that of the wild-type enzyme (Fig. 4B, the isolated product yield reached 53.23%). Kinetic analysis revealed that the NovO (I6V/C47G) mutant exhibits comparable k_{cat} values for SAM and CPM-SAM, while its K_M is reduced by a factor of 16 (Table S3).

O-Methyltransferases (OMTs), the largest class of methyltransferases in nature, play critical roles in natural product biosynthesis.[32] DnrK catalyzes the 4-*O*-methylation of carminomycin in the biosynthesis of the antitumor drug daunorubicin.[33] We investigated the activity of the *Acl*HMT (FIDF)–DnrK cascade for the 4-*O*-cyclopropylmethylation of carminomycin (**7**, Fig. 5). However, wild-type DnrK exhibited no detectable activity toward CPM-SAM (Fig. S12). Structural analysis of DnrK with SAH bound (PDB: 1TW2) revealed two bulky residues, F156 and L160, positioned near the sulfur atom (Fig. S11A). Molecular docking simulations demonstrated that L160 acts as a steric barrier, preventing the cyclopropylmethyl group of CPM-SAM from accessing the 4-OH of the substrate (Fig. S11B). Inspired by our previous design of the DnrK (L160A) mutant for FEt-SeAM,[21] we conducted docking studies with CPM-SAM. These simulations revealed that the L160A mutation alleviates steric hindrance, positioning the cyclopropylmethyl moiety near the catalytic site properly. Subsequent activity assays using *Acl*HMT (FIDF)–DnrK (L160A) confirmed the production of 4-*O*-cyclopropylmethylated carminomycin (**8**), with a yield of 54.76% (Fig. 5B, 51.3% isolated yield). To further optimize the efficiency, we introduced the double mutants F156A, L, and S/L160A. However, the catalytic performance remained inferior to that of the single mutant DnrK (L160A).

Flavonoids are key phenolic compounds with therapeutic potential against cancer, oxidative stress, pathogens, inflammation, and cardiovascular dysfunction.[34] However, poor stability *in vivo* limits their clinical use. Research showed that O-methylation enhances their lipophilicity and stability, improving their potential as pharmaceutical agents for new applications.[35,36] ROMT9, an *O*-methyltransferase from *Oryza*
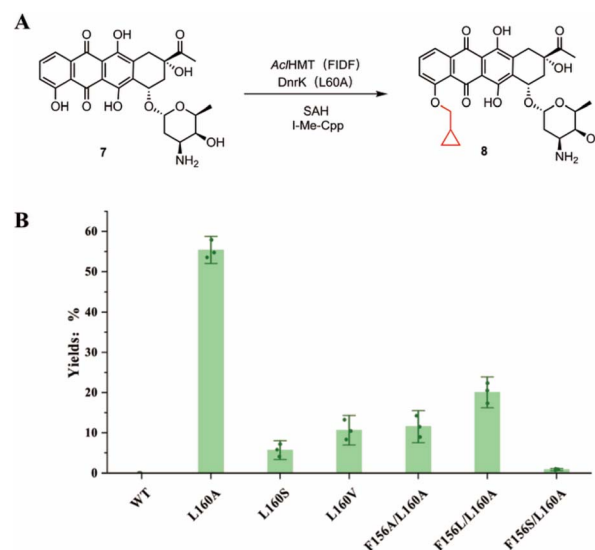

Fig. 5 (A) Cyclopropylmethylation activity of the *Acl*HMT (FIDF)–Dnrk (L160A) cascade reactions. The *Acl*HMT (FIDF)–Dnrk (L160A) assay contained 80 μM SAH, 3 mM I-Me-Cpp, 1 mM substrate (**7**), 40 μM *Acl*HMT (FIDF) and 80 μM Dnrk (L160A) in 50 mM Tris–HCl (pH 8.0), and the solution was incubated at 30 °C for 24 h. (B) Activity summary of *Acl*HMT (FIDF)–DnrKs cascade reactions with DnrK mutants. The data plotted are the means of three independent measurements with standard deviation.

sativa subsp. *Japonica*, specifically catalyzes the 3′-*O*-methylation of eriodictyol (**9**) to produce homoeriodictyol, a compound exhibiting antioxidant, anti-inflammatory, antimicrobial, and
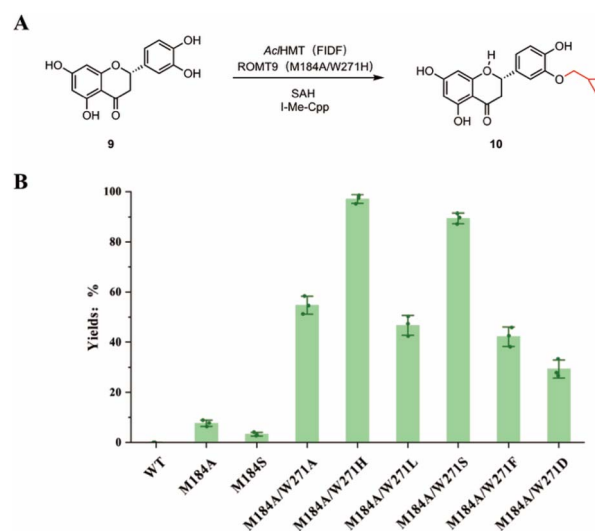

Fig. 6 (A) Cyclopropylmethylation activity of the *Acl*HMT (FIDF)–ROMT9 (M184A/W271H) cascade reactions. The *Acl*HMT (FIDF)–ROMT9 (M184A/W271H) assay contained 80 μM SAH, 3 mM I-Me-Cpp, 1 mM substrate (**9**), 40 μM *Acl*HMT (FIDF) and 80 μM ROMT9 (M184A/W271H) in 10 mM Tris–HCl at pH 8.0, and the solution was incubated at 30 °C for 24 h. (B) Activity summary of *Acl*HMT (FIDF)–ROMT9 cascade reactions with ROMT9 mutants. The data plotted are the means of three independent measurements with standard deviation.

© 2025 The Author(s). Published by the Royal Society of Chemistry

anticancer activities.[37] We evaluated the *Acl*HMT (FIDF)–ROMT9 cascade system for the 3′-*O*-cyclopropylmethylation of eriodictyol (**9**, Fig. 6 and S14). Again, the wild-type ROMT9 failed to recognize CPM-SAM. Since the crystal structure of ROMT9 remains unresolved, molecular docking of SAH into the AlphaFold-predicted structure (AF-Q6ZD89-F1) identified residue M184 (4.0 Å from the sulfur atom) as potential steric hindrance (Fig. S13A). Docking simulations with CPM-SAM revealed positional inconsistency compared with SAH binding (Fig. S13B), suggesting that M184 obstructs CPM-SAM accommodation. To alleviate steric clashes, we engineered M184 to smaller residues (Ala/Ser). Activity assays confirmed that both mutants acquired catalytic activity on CPM-SAM, with M184A exhibiting a 7.75% product yield (Fig. 6B and S14). W271, a bulky aromatic residue near the binding site, was further optimized. Systematic mutagenesis of W271 to smaller residues (Ala, His, Leu, Ser, and Val) identified ROMT9 (M184A/W271H) as the most efficient variant with a 97.41% yield for cyclopropymethylated eriodictyol (Fig. 6B). Docking of CPM-SAM with the ROMT9 double mutant (M184A/W271H) demonstrated perfect overlap with the original SAH position (Fig. S13C). Kinetic analysis revealed that the ROMT9 (M184A/W271H) mutant exhibits closely matched k_{cat} and K_M values for SAM and CPM-SAM (Table S3).

Moreover, the cyclopropylmethylation reactions using CPM-SAM directly and the *Acl*HMT (FIDF)–MT coupled enzymatic cascade were compared using all the top-performing mutants of the methyltransferases mentioned above. Although direct catalysis resulted in marginally higher reaction rates during the initial 3–12 h, the coupled enzymatic system ultimately achieved superior product yields (Fig. S6–S14). This strategy not only reduces the consumption of costly SAH but also enhances production efficiency, demonstrating its practical advantage for scalable biosynthesis.

Conclusions

In summary, we successfully synthesized a cyclopropylmethyl-SAM analogue (CPM-SAM) using engineered *Acl*HMT (FIDF). Through enzyme engineering, we enhanced the catalytic efficiency of diverse methyltransferases (MTs) toward CPM-SAM, particularly transforming several MTs that were initially incapable of recognizing CPM-SAM into highly efficient cyclopropylmethyl transferases. By coupling *Acl*HMT (FIDF)-mediated *in situ* CPM-SAM synthesis with engineered MTs, we achieved enzymatic cyclopropylmethylation across *N*-, *S*-, *C*-, and *O*-nucleophilic sites. This strategy provides a sustainable and selective platform for generating cyclopropylmethyl-containing analogues of bioactive molecules in a late-stage manner, offering green biocatalysts for pharmaceutical discovery and diversification.

Author contributions

H. Z., N. Y. and S. W. performed the experiments. H. Z. interpreted the data and wrote the initial manuscript. M. D. supervised the project and edited the manuscript.

Conflicts of interest

There are no conflicts to declare.

Data availability

All experimental procedures, kinetic and NMR data are available in the supplementary information (SI). See DOI: https://doi.org/10.1039/d5sc06767g.

Acknowledgements

Notes and references

1 K. W. Bentley and D. G. Hardy, *J. Am. Chem. Soc.*, 1967, **89**, 3281–3292.

2 A. C. Pierce, G. Rao and G. W. Bemis, *J. Med. Chem.*, 2004, **47**, 2768–2775.

3 G. Rai, D. J. Urban, B. T. Mott, X. Hu, S.-M. Yang, G. A. Benavides, M. S. Johnson, G. L. Squadrito, K. R. Brimacombe, T. D. Lee, D. M. Cheff, H. Zhu, M. J. Henderson, K. Pohida, G. A. Sulikowski, D. M. Dranow, M. Kabir, P. Shah, E. Padilha, D. Tao, Y. Fang, P. P. Christov, K. Kim, S. Jana, P. Muttil, T. Anderson, N. K. Kunda, H. J. Hathaway, D. F. Kusewitt, N. Oshima, M. Cherukuri, D. R. Davies, J. P. Norenberg, L. A. Sklar, W. J. Moore, C. V. Dang, G. M. Stott, L. Neckers, A. J. Flint, V. M. Darley-Usmar, A. Simeonov, A. G. Waterson, A. Jadhav, M. D. Hall and D. J. Maloney, *J. Med. Chem.*, 2020, **63**, 10984–11011.

4 Å. Rosenquist, B. Samuelsson, P.-O. Johansson, M. D. Cummings, O. Lenz, P. Raboisson, K. Simmen, S. Vendeville, H. De Kock, M. Nilsson, A. Horvath, R. Kalmeijer, G. De La Rosa and M. Beumont-Mauviel, *J. Med. Chem.*, 2014, **57**, 1673–1693.

5 A. Chaturbedi, J. Mann, S. Chakravartula, B. Thrasher, G. Arabidarrehdor, J. Zirkle, H. Meshkin, S. C. Nallani, J. Florian and Z. Li, *Clin. Pharmacol. Ther.*, 2025, **117**, 836–845.

6 V. A. Beltrami, F. R. B. Martins, D. G. Martins, C. M. Queiroz-Junior, F. B. Félix, L. C. Resende, F. R. D. S. Santos, L. D. S. B. Lacerda, V. R. D. M. Costa, W. N. Da Silva, P. P. G. Guimaraes, G. Guimaraes, F. M. Soriani, M. M. Teixeira, V. V. Costa and V. Pinho, *Inflammation Res.*, 2025, **74**, 24.

7 W. P. Blackaby, R. T. Lewis, J. L. Thomson, A. S. R. Jennings, S. C. Goodacre, L. J. Street, A. M. MacLeod, A. Pike, S. Wood, S. Thomas, T. A. Brown, A. Smith, G. Pillai, S. Almond, M. R. Guscott, H. D. Burns, W. Eng, C. Ryan, J. Cook and T. G. Hamill, *ACS Med. Chem. Lett.*, 2010, **1**, 350–354.

8 X. Tong, W. Keung, L. D. Arnold, L. J. Stevens, A. J. Pruijssers, S. Kook, U. Lopatin, M. Denison and A. D. Kwong, *Antimicrob. Agents Chemother.*, 2023, **67**, e00840.

9 W. Wu, Z. Lin and H. Jiang, *Org. Biomol. Chem.*, 2018, **16**, 7315–7329.

10 S. Peraka, A. Hussain and D. B. Ramachary, *J. Org. Chem.*, 2018, **83**, 9795–9817.

11 A. L. Gabbey, K. Scotchburn and S. A. L. Rousseaux, *Nat. Rev. Chem.*, 2023, **7**, 548–560.

12 C. Liao and F. P. Seebeck, *Nat. Catal.*, 2019, **2**, 696–701.

13 I. R. Bothwell and M. Luo, *Org. Lett.*, 2014, **16**, 3056–3059.

14 E. Abdelraheem, B. Thair, R. F. Varela, E. Jockmann, D. Popadić, H. C. Hailes, J. M. Ward, A. M. Iribarren, E. S. Lewkowicz, J. N. Andexer, P. Hagedoorn and U. Hanefeld, *ChemBioChem*, 2022, **23**, e202200212.

15 A. Hoffmann, K. H. Schülke, S. C. Hammer, A. Rentmeister and N. V. Cornelissen, *Chem. Commun.*, 2023, **59**, 5463–5466.

16 J. Peng, G. R. Hughes, M. M. Müller and F. P. Seebeck, *Angew. Chem., Int. Ed.*, 2024, **63**, e202312104.

17 L. Kong, J. Zhang, H. Wang, Z. Wei, W. Wang, J. Hu and M. Dong, *Angew. Chem., Int. Ed.*, 2025, **64**, e202419815.

18 W. Wang, H. Zhao, N. Yu, F. Chen and M. Dong, *ACS Catal.*, 2023, **13**, 13729–13734.

19 J. Peng, C. Liao, C. Bauer and F. P. Seebeck, *Angew. Chem., Int. Ed.*, 2021, **60**, 27178–27183.

20 S. S. Neti, B. Wang, D. F. Iwig, E. L. Onderko and S. J. Booker, *ACS Cent. Sci.*, 2023, **9**, 905–914.

21 N. Yu, H. Zhao, W. Wang and M. Dong, *ACS Catal.*, 2024, **14**, 6211–6216.

22 W. Ding, M. Zhou, H. Li, M. Li, Y. Qiu, Y. Yin, L. Pan, W. Yang, Y. Du, X. Zhang, Z. Tang and W. Liu, *Org. Lett.*, 2023, **25**, 5650–5655.

23 Q. Tang, C. W. Grathwol, A. S. Aslan-Üzel, S. Wu, A. Link, I. V. Pavlidis, C. P. S. Badenhorst and U. T. Bornscheuer, *Angew. Chem., Int. Ed.*, 2021, **60**, 1524–1527.

24 K. H. Schülke, J. S. Fröse, A. Klein, M. Garcia-Borràs and S. C. Hammer, *ChemBioChem*, 2024, **25**, e202400079.

25 W. Zhang, G. Rong, J. Gu, C. Fan, T. Guo, T. Jiang, W. Deng, J. Xie, Z. Su, Q. Yu, J. Mai, R. Zheng, X. Chen, X. Tang and J. Zhang, *FASEB J.*, 2022, **36**, e22084.

26 S. Coulthard and L. Hogarth, *Invest. New Drugs*, 2005, **23**, 523–532.

27 H. Wu, J. R. Horton, K. Battaile, A. Allali-Hassani, F. Martin, H. Zeng, P. Loppnau, M. Vedadi, A. Bochkarev, A. N. Plotnikov and X. Cheng, *Proteins: Struct., Funct., Bioinf.*, 2007, **67**, 198–208.

28 N. V. Cornelissen, R. Mineikaitė, M. Erguven, N. Muthmann, A. Peters, A. Bartels and A. Rentmeister, *Chem. Sci.*, 2023, **14**, 10962–10970.

29 G. Anywar and E. Muhumuza, *Front. Pharmacol.*, 2024, **14**, 1231006.

30 J. C. Sadler, C. H. Chung, J. E. Mosley, G. A. Burley and L. D. Humphreys, *ACS Chem. Biol.*, 2017, **12**, 374–379.

31 O. Khersonsky, R. Lipsh, Z. Avizemer, Y. Ashani, M. Goldsmith, H. Leader, O. Dym, S. Rogotner, D. L. Trudeau, J. Prilusky, P. Amengual-Rigo, V. Guallar, D. S. Tawfik and S. J. Fleishman, *Mol. Cell*, 2018, **72**, 178–186.

32 T. Grocholski, P. Dinis, L. Niiranen, J. Niemi and M. Metsä-Ketelä, *Proc. Natl. Acad. Sci. U. S. A.*, 2015, **112**, 9866–9871.

33 A. Jansson, H. Koskiniemi, P. Mäntsälä, J. Niemi and G. Schneider, *J. Biol. Chem.*, 2004, **279**, 41149–41156.

34 S. Alseekh, L. Perez De Souza, M. Benina and A. R. Fernie, *Phytochemistry*, 2020, **174**, 112347.

35 Y. Liu, A. R. Fernie and T. Tohge, *Plants*, 2022, **11**, 564.

36 N. Koirala, N. H. Thuan, G. P. Ghimire, D. V. Thang and J. K. Sohng, *Enzyme Microb. Technol.*, 2016, **86**, 103–116.

37 H. C. Erythropel, J. B. Zimmerman, T. M. De Winter, L. Petitjean, F. Melnikov, C. H. Lam, A. W. Lounsbury, K. E. Mellor, N. Z. Janković, Q. Tu, L. N. Pincus, M. M. Falinski, W. Shi, P. Coish, D. L. Plata and P. T. Anastas, *Green Chem.*, 2018, **20**, 1929–1961.